

Florent Xavier Gadéa · Thierry Leininger

# Accurate *ab initio* calculations for LiH and its ions, $\text{LiH}^+$ and $\text{LiH}^-$

Received: 2 January 2005 / Accepted: 15 September 2005 / Published online: 22 February 2006  
© Springer-Verlag 2006

**Abstract** *Ab initio* calculations were performed for LiH using a pseudopotential approach with CPP corrections and huge basis sets on both atoms. A wide range of  $1,3\Sigma^+$  electronic adiabatic states have been investigated, from the ground state up to those dissociating into  $\text{Li}(5p)+\text{H}$ . Permanent and transition electric dipole moments are also considered for the first few excited states. Comparison with experiments and recent all-electron calculations, reveals an excellent global accuracy, only the bottom of the ground state being better described by all-electron approaches. Using almost identical basis sets, coupled cluster all-electron calculations are performed for the ground states of  $\text{LiH}^+$ ,  $\text{LiH}^-$  and LiH. High care has been given to the correct relative position of the asymptotes, allowing for this rather complete set of accurate *ab initio* data to be useful for further molecular physics studies.

## 1 Introduction

As the simplest heteroatomic molecule, LiH has aroused since a long time considerable interest, which still goes on, mainly from theoreticians, but also from experimentalists. Despite its apparent simplicity, many of the interesting challenges of quantum chemistry can be addressed in LiH. One example is the treatment of the core, which can be considered either explicitly in all-electron approaches, or through a pseudopotential approach that may be improved to account for the core valence correlation. Furthermore, this fascinating molecule is ionic at equilibrium geometries, with a strong dipole moment, but dissociates to a neutral asymptote. Therefore an important change occurs in the electronic states as the

F.X. Gadéa (✉)  
Groupe NanoScience (GNS), CEMES, UPR 8011 du CNRS,  
29 rue J. Marvig, BP 4347, 31055 Toulouse Cedex, France  
E-mail: gadea@irsamc.ups-tlse.fr

F.X. Gadéa · T. Leininger  
Laboratoire de Physique Quantique, UMR 5626, IRSAMC,  
Université Paul Sabatier, 118, route de Narbonne,  
31062 Toulouse Cedex 4, France  
E-mail: Thierry.Leininger@irsamc.ups-tlse.fr

internuclear distance increases. This change makes this system suitable to test the ability of *ab initio* approaches to deal with multireference state and also to test diabatisation procedures for which the physical insights should be preserved and the electronic coupling determined between ionic and neutral states as it is the case here. From the spectroscopical point of view, LiH is also an interesting molecule, with very unusual shapes of the potential energy surfaces (PES), far from harmonic or Morse behaviours. Flat bottomed, as the first excited (*A*) or double wells PES, as the *C* and *D* states, are the rule here rather than the exception [1–7].

LiH is thus often used for benchmark calculations and many improvements in *ab initio* calculations have been tested on this molecule [8–10, 3, 4, 11, 12]. Lithium hydride is also an important molecule for astrophysics as it imprints the chemistry of the early universe [13–18] where the various mechanisms of its formation and decay are investigated. These mechanisms often involve the ionic species  $\text{LiH}^+$  or  $\text{LiH}^-$  and the interactions with photons or electrons (radiative association, dissociative recombination, dissociative attachment, reactive collisions, etc.). LiH and its ions are thus molecules of paramount importance in various fields of chemistry, physics or astrophysics [1–55].

Despite this great interest, a comprehensive theoretical study is still missing, most of the contributions concentrating on a given specific point. It is the aim of this paper to present a high quality global approach for LiH in  $1\Sigma^+$  and  $3\Sigma^+$  symmetries, including ground and excited states up to  $5p$ , and for the ground states of its anion ( $\text{LiH}^-$ ) and cation ( $\text{LiH}^+$ ). Recent progress in all-electron approaches have led to renewed interest but focussed mainly on the bottom of the well. It is interesting to compare these results to the present more conventional pseudopotential study which allows larger basis sets to be used.

## 2 Theory

All the present calculations have been performed with the MOLPRO package [19], using various large basis sets and

**Table 1** Atomic spectrum of Li (in  $\text{cm}^{-1}$ )

	Abs. energies (a.u.)	$\Delta E$ (theo.)	$\Delta E$ (exp.) <sup>a</sup>	Error
2s	-0.19811767	0	0	
2p	-0.13023525	14898.47	14903.89	-5.42
3s	-0.07417795	27201.62	27206.12	-4.50
3p	-0.05723562	30920.04	30925.38	-5.34
3d	-0.05560115	31278.76	31283.10	-4.34
4s	-0.03861622	35006.52	35012.06	-5.44
4p	-0.03197273	36464.60	36469.55	-4.95
4d	-0.03123921	36625.59	36623.39	2.20
4f	-0.03119850	36634.52	36630.20	4.32
5s	-0.02363719	38294.04	38299.50	-5.46
5p	-0.02036033	39013.23	39015.56	-2.33
Li <sup>+</sup>	0	43481.80	43487.19	-5.39

<sup>a</sup> Experimental from Ref. [21]

various approaches, either with all the electrons or with a pseudopotential for the lithium core ( $1s^2$ ) together with its usual core polarisation potential (CPP) [20] to account for the core valence correlation. This CPP uses a single parameter fitted to reproduce the experimental ionisation potential of Li. For LiH all the states dissociating below the  $\text{Li}(5p)+\text{H}(1s)$  asymptote were considered, therefore all the states dissociating below the ionic asymptote are investigated. Very large atomic basis sets ( $27s17p14d6f2g$  for Li, and,  $20s11p7d4f2g$  for H) have been used, and a full valence configuration interaction (CI) in the pseudopotential and CPP approaches was performed. The lithium atomic spectrum is compared in Table 1 with the experimental one [21]. As can be seen, the errors are of the order of a few wavenumbers, for the whole spectrum. For  $\text{LiH}^+$ , a basis set of similar quality has been used, but without some of the specific Rydberg gaussian functions. Initially optimised to get accurate scattering length for the lowest triplet state of LiH (the recommended values for the different isotopomers have been estimated with an accuracy of  $\pm 5$ –10%) [22], it yields accurate atomic energies and low-lying spectrum, as well as polarisabilities or electron affinities (see reference [22] for details). All-electron calculations at the CCSD(T) level have been performed for  $\text{LiH}^+$ . For the sake of comparison of the various ground states, all-electron calculations at the CCSD(T) level with the same basis set than for  $\text{LiH}^+$  have also been performed for LiH and  $\text{LiH}^-$ .

### 3 LiH

#### 3.1 Potential energy curves and spectroscopy

There are various interesting aspects in the potential energy curves of LiH. The interplay between ionic and neutral states for the  $^1\Sigma^+$  symmetry is known since a long time and has been nicely revealed by the diabatic study developed in our group [3, 23–25]. The behaviour of the Rydberg curves which present oscillations both for singlet and triplet  $\Sigma$  symmetries is also very interesting. The spectroscopy of the ground ( $X$ ) and first excited ( $A$ ) states has been intensively studied and

is experimentally well established. It has been reviewed in reference [1]. The investigation of the higher states C and D is more recent [6, 7, 26–29]. Most of the vibrational levels of the C state [26, 28, 29] and many of the D [27] state have been observed using two photon spectroscopy.

For the ground state, a large number of calculations have been published, either motivated by methodological or physical guidelines. The best theoretical results were obtained by a recent all-electron full CI study that will be used to compare with the present data. For the higher excited states, A, C and D, theoretical studies are scarce and we will concentrate on a comparison with experimental results. We have split the presentation of the  $^1,3\Sigma^+$  in four figures, using two criteria, singlet or triplet spin symmetry, and low or high lying in energy. Figures 1 and 2 illustrate the low lying states of singlet and triplet symmetry, respectively, Figs. 3 and 4 the high-lying singlets and triplets as well as the potential curve of  $\text{LiH}^+$ . The calculations have been performed for a very large number of internuclear distances, as can be noticed by the symbols on some selected curves only, for the sake of clarity. A particular care has been taken to have a high enough density of calculated points around all avoided crossings. Although the curves have not been interpolated, they look quite smooth.

Figure 1 shows the adiabatic  $^1\Sigma^+$  potentials X, A, C, D and the ones dissociating to  $n=3$  ( $3s$  and  $3p$ ). The ionic curve behaves roughly as  $1/R$ ; it lies above the  $n=3$  curves at larger internuclear distances ( $R=45$  a.u.) and crosses all the lower-lying neutral states with increasingly avoided crossings as the bond length decreases. The X state is thus ionic at equilibrium and dissociates to a neutral state to the  $2s$  asymptote. The A state is flat bottomed because of the largely avoided crossing around  $R=7$  a.u. between the ionic and the repulsive  $2s$  state. The C state presents two minima, one at about  $R=10$  a.u. resulting from the avoided crossing between the ionic and the neutral  $2p$  states, and another one at shorter distance and higher energy. The D state also presents two minima, one at large distance related to the ionic–neutral ( $3s$ ) avoided crossing, and another at short distance which could be related to an avoided crossing between two neutral states, an attractive short range  $3s$  and a repulsive  $2p$ .

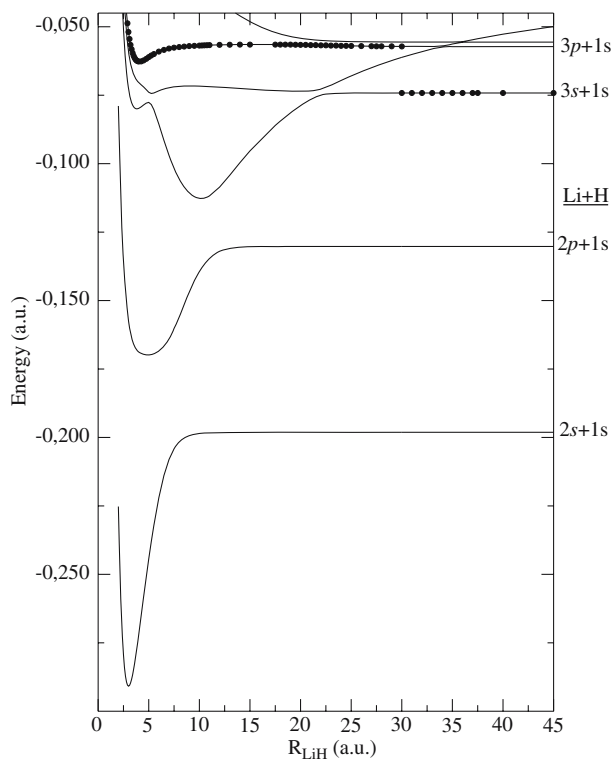


**Fig. 1** Low-lying  $^1\Sigma^+$  states of LiH

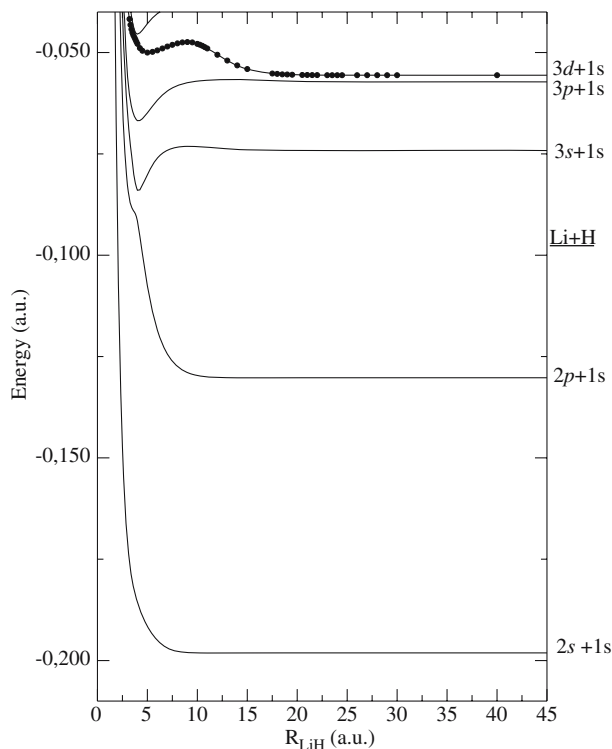


**Fig. 2** Low-lying  $^3\Sigma^+$  states of LiH

These various avoided crossings, often imprinted, but not only, by the ionic state, lead to quite unusual shapes for the potential energy curves and their spectroscopy. The A, C and

*D* curves can be hardly approximated by the usual harmonic or Morse functions.

The low lying  $^3\Sigma^+$  curves are plotted in Figure 2. The lowest curves are essentially repulsive, while some similarity with the curve of the  $\text{LiH}^+$  ion appears from the lowest curve dissociating to  $n = 3(3s)$ .

Based on a powerful diabatic approach, the only one to our knowledge able to determine diabatic states at short distances, a detailed analysis of these neutral–ionic and neutral–neutral interactions was performed previously [3,4,23, 24,30–32]. This study has revealed the overrepulsivity of the lowest neutral states generating series of crossings at short distances hidden by large couplings, in addition to the neutral–ionic crossings at larger distances. However, this diabatic approach forbids the use of huge basis sets and therefore leads to limited accuracy, although this limitation can be to a large extent compensated by specific corrections (for example, to the ionic diabatic energy).

Singlet and triplet adiabatic potential curves dissociating to  $3p$  through  $5p$  are reported in Figs. 3 and 4, respectively, together with the  $\text{LiH}^+$  curve. For both symmetries one can see two kinds of behaviour, flat curves like  $3p$ ,  $4s$ ,  $4p$ ,  $4d$ ,  $5s$  and  $5p$ , and repulsive ones like  $3d$  and  $4f$ . Oscillations are obvious in the repulsive curves and also, but at a smaller scale, in almost all curves, particularly when they are energetically well separated from the others. These oscillations are magnified by the diabatic approach and were related to the amplitude of the corresponding Rydberg orbital [3]. A striking effect is that the repulsive curves for singlet and triplet

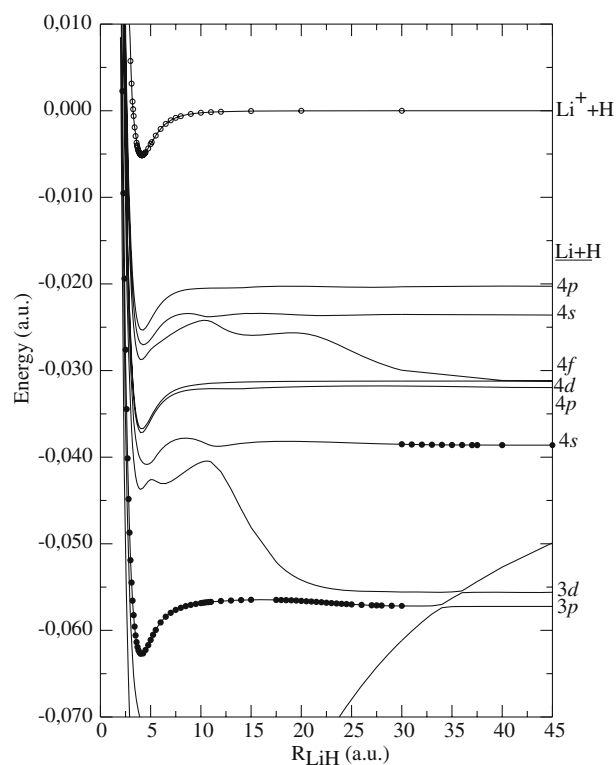


**Fig. 3** High-lying  $^1\Sigma^+$  states of LiH

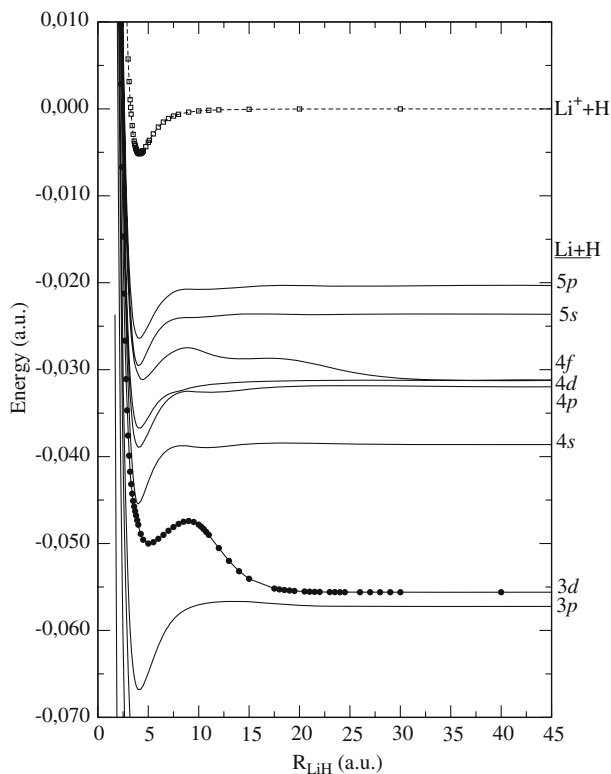


**Fig. 4** High-lying  ${}^3\Sigma^+$  states of LiH

states have a similar shape but with a larger amplitude in the case of singlets. It is also worth noticing that these repulsive curves emerge from a block of asymptotically quasidegenerate curves, converging to the same  $n$ . As shown in [32,33], these behaviours are nicely explained by the Fermi model, where the potential is predicted to be proportional to the scattering length of an electron colliding with the hydrogen atom and to the atomic amplitude of the Rydberg lithium function experimented by the hydrogen atom. Since this scattering length is positive, we have repulsive effects; and since it is much smaller for triplet than for singlet, the global behaviour is the same but with a larger amplitude for the singlet curves. Noteworthy, for nearly degenerate states, the model predicts only flat curves except for one which behaves like the trace of the interaction matrix. This is exactly what we see here, for the nearly degenerate  $3p - 3d$  block, flat curves and a repulsive one, much more repulsive for singlet than for triplet, and also for the  $4p - 4d - 4f$  block. This behaviour emphasises an important  $l$  mixing between the underlying diabatic curves in case of asymptotic neardegeneracy. At short distances, for  $n = 3$ , the magnitude of the interaction is so large that the repulsive  $n = 3$  curve crosses the attractive  $4s$  curve, producing  $n$  mixing, two avoided crossings and very unusual shapes for the adiabatic curves  $F$  and  $G$ . These behaviours are not artefacts, the wells actually trapping vibrational levels which could possibly be observed, although important vibronic effects at least as large as for the  $C$  and  $D$  states [6,7] should be expected here.

Spectroscopic data of interest are reported in Tables 2, 3 and 4. Table 2 is devoted to the binding energy ( $D_e$ ) and equilibrium distance ( $R_e$ ) and  $G_0$  for the  $X$ ,  $A$ ,  $C$  and  $D$  states. The corresponding experimentally known data for these states is also reported in Table 2, for comparison. The agreement between our computed data and the experimental one is good for the  $X$  state, better for the  $A$  state and becomes excellent for the  $C$  state. Since our equilibrium distance is too short, the discrepancy for the  $X$  state is probably due to some lack of repulsive effects related to the pseudopotential approach.

A deeper comparison can be performed from inspection of the vibrational spacings. They are reported in Table 3 for the  $X$  and  $A$  states, and in Table 4 for the  $C$  and  $D$  ones, together with the most accurate ab initio results for the  $X$  state and the experimental ones for the  $X$ ,  $A$ ,  $C$  and  $D$  states. The agreement between the theoretical spacing of Lundsgaard and Rudolph [34] and the experimental one is impressive for the lowest vibrational levels, showing that all-electron full CI approaches can yield excellent accuracy. However for such approaches, the basis set has to be restricted and substantial errors in the electron affinity (EA) of H ( $273\text{ cm}^{-1}$ ) and in the ionisation potential (IP) of Li ( $34\text{ cm}^{-1}$ ) remain. As a consequence, their ionic asymptote is in error by about  $240\text{ cm}^{-1}$  and, as analysed previously [3], this error is reflected in their error for the binding energy of the ground state ( $182\text{ cm}^{-1}$ ). We used much larger basis set for H leading to a better description of  $\text{H}^-$  and thus an improved EA (only  $15\text{ cm}^{-1}$  in error) and the use of CPP allows to an almost exact IP for Li, therefore our ionic asymptote is better positioned with respect to the neutral lowest dissociation limit [ $\text{Li}(2s)+\text{H}(1s)$ ], and our binding energy of the ground state is in error by  $64\text{ cm}^{-1}$  only. As a consequence, when  $v$  increases, the agreement with the experimental spacing rapidly deteriorates in Lundsgaard's calculation while it improves in ours, the inversion occurring for  $v = 10$ .

For the  $A$  state, it was shown that the quality of the ionic state is crucial for all the vibrational spacings, since it controls the global width of the well [3]. We get here a slight underestimation for all  $v$  with respect to the experimental spacing. However, our present results correspond to the best ab initio determination without any correction. This underestimation is larger for the lowest  $v$  and could be related either to the ionic state at larger distance or again to some lack of repulsive effects at short distances.

Vibronic effects have been evaluated in previous studies taking benefit of the diabatic approach. Although they produce increasing shifts as the energy increases, these vibronic shifts remain rather similar for all the vibrational levels of the  $X$  and  $A$  states [5,35] and for the lower part of the  $C$  state [6], therefore not affecting much the vibrational spacing except for the higher part of the  $C$  state and for many levels in the  $D$  state [7]. Noteworthy, as can be seen in Table 3, the agreement between our theoretical vibrational spacing and the experimental one, is excellent for almost all vibrational levels of the  $C$  state, from  $v = 0$  to  $v = 42$ . The deviation is often about  $10^{-2}\text{ cm}^{-1}$ , therefore within the vibronic effects on the

**Table 2** Spectroscopic constants of the low-lying  $^1\Sigma^+$  states of LiH

	$X^1\Sigma^+$		$A^1\Sigma^+$		$C^1\Sigma^+$	$D^1\Sigma^+$	
$R_e$ (a.u.)	3.003	3.015 <sup>a</sup>	4.862	4.906 <sup>a</sup>	3.821 (10.181*)	(10.140 <sup>b*</sup> )	5.280 (19.824*)
$D_e$ (eV)	2.523	2.515 <sup>a</sup>	1.077	1.076 <sup>a</sup>	1.048	1.050 <sup>b</sup>	0.464
$G_0$ (cm <sup>-1</sup> )	695.7	697.9 <sup>a</sup>	130.0	131.3 <sup>a</sup>	146.6	146.7 <sup>b</sup>	108.4

\* outer well value

<sup>a</sup> Experimental values from Ref.[1]<sup>b</sup> Experimental values from Ref.[27]**Table 3** Spacings (in cm<sup>-1</sup>),  $\Delta G_v^+$ , between the vibrational levels of the low-lying  $X$  and  $A^1\Sigma^+$  states of LiH

$v$	$X^1\Sigma^+$			$A^1\Sigma^+$	
	This work	Lundsgaard and Rudolph <sup>a</sup>	Chan et al. <sup>b</sup>	This work	Way and Stwalley <sup>c</sup>
0	1355.81	1359.66	1359.71	278.43	280.84
1	1311.43	1314.68	1314.89	310.93	312.97
2	1267.93	1270.55	1270.89	333.96	335.69
3	1225.25	1227.31	1227.77	351.32	352.79
4	1183.28	1184.87	1185.44	364.47	365.85
5	1141.93	1143.06	1143.77	374.40	375.60
6	1101.05	1101.72	1102.60	381.70	382.68
7	1060.46	1060.73	1061.78	386.58	387.55
8	1020.00	1019.88	1021.17	389.59	390.37
9	979.43	978.85	980.52	390.79	391.59
10	938.43	937.40	939.62	390.37	391.05
11	896.77	895.21	898.09	388.55	389.19
12	854.04	851.75	855.48	385.33	385.94
13	809.68	806.39	811.19	380.82	381.32
14	763.20	758.32	764.44	375.02	375.21
15	713.69	706.47	714.22	367.88	
16	660.02	649.46	659.27	359.31	
17	600.82	585.5	597.89	349.11	
18	533.93	512.3	527.91	337.00	
19	456.87	427.12	446.61	322.47	
20	366.46	326.95	350.99	304.78	
21	259.59	209.30	237.71	282.75	
22		76.29		254.54	
23				217.49	
24				166.72	

<sup>a</sup> Theoretical results from Ref. [34]<sup>b</sup> Experimental values from Ref. [49]<sup>c</sup> Experimental values from Ref. [55]

vibrational spacing. Moreover, when there is a large discrepancy,  $-12.5\text{ cm}^{-1}$  for  $v = 38$ , the error is consistent with the vibronic correction ( $-11.7\text{ cm}^{-1}$ ) [6] both in sign and magnitude. The position of the  $v = 34$  level, located in the inner well, is very sensitive to a delicate balance between the various interactions. Even without any correction, we obtain it at the right place between the  $v = 33$  and  $v = 35$  levels of the main well, but somewhat below the experimental position. It should be emphasised that we get all the vibrational levels below  $v = 30$ , where vibronic effects on the vibrational spacing are very small (of the order of  $10^{-2}\text{ cm}^{-1}$ ), with an accuracy much below the wavenumber, and in fact almost all below the tenth of a wavenumber. This remarkable accuracy illustrates the quality of our description of the ionic and neutral states and of the avoided crossings. It clearly shows that our calculation presents some deficiencies only at very short

distances, otherway it yields a previously unattained accuracy, predicting the position of almost all vibrational levels of the  $C$  state within a tenth of a wavenumber.

For the  $D$  state, the comparison with the experimental spacing is more involved because the observed levels are scarce and vibronic effects become important [7]. In particular the lowest level of the inner well has not yet been observed and presents a strong vibronic shift [7]. This level is labelled  $v = 1$ , since it is expected between the lowest ( $v = 0$ ) and the first excited ( $v = 2$ ) levels of the outer and main well. Here, within a Born–Oppenheimer approach, we found it below  $v = 0$ , as in [7] without vibronic corrections. The experimental spacing varies quite erratically. Going up in  $v$ , there is a global decrease up to  $v = 7-8$  and then an increase, but with several exceptions. This strange behaviour is related to the unusual shape of the wells and to, strong vibronic effects.

**Table 4** Spacings (in  $\text{cm}^{-1}$ ),  $\Delta G_v^+$  between the vibrational levels of the low-lying  $C$  and  $D^1\Sigma^+$  states of LiH

$v$	$C^1\Sigma^+$		$D^1\Sigma^+$	
	This work	Exp. <sup>a</sup>	This work	Exp. <sup>b</sup>
0	290.98	290.99	-8.71 ( $v = 1$ )	
1	286.56	286.42	58.07 ( $v = 0$ )	59.27
2	281.93	281.79	58.35	56.81
3	277.22	277.13	57.83	59.74
4	272.57	272.44	56.64	57.19
5	267.92	267.73	42.94	
6	263.25	269.03	11.68	
7	258.50	258.31	51.39	11.20
8	253.75	253.63	44.24	40.31
9	249.08	248.95	25.58	
10	244.45	244.33	32.36	
11	239.84	239.72	41.60	45.47
12	235.26	235.17	44.64	41.11
13	230.74	230.67	47.82	44.78
14	226.27	226.21	50.71	58.08
15	221.85	221.81	53.29	58.06
16	217.48	217.48	55.63	
17	213.18	213.19	57.78	
18	208.96	205.98	59.78	73.61
19	204.80	204.81	61.65	67.12
20	200.71	200.71	63.38	
21	196.66	196.67	64.99	
22	192.67	192.68	66.48	
23	188.72	188.73	67.84	79.92
24	184.81	184.84	69.07	77.33
25	180.92	180.97	70.16	
26	177.07	177.16	71.14	
27	173.23	173.35	72.00	
28	169.39	169.57	72.74	
29	165.50	165.80	73.36	
30	161.48	162.02	73.90	
31	157.16	158.23	74.34	
32	151.11	153.30	74.68	
33	63.15	96.93	74.94	
34	89.01	54.83	75.12	
35	139.21	142.12	75.23	
36	126.44	132.27	75.27	
37	102.62	103.67	75.24	
38	99.27	86.77	75.15	
39	113.65	112.6	74.99	
40	114.42	116.50	74.79	
41	105.79	106.24	74.53	
42	85.09	84.51	74.22	
43			73.87	
44			73.48	
45			73.05	
46			72.58	
47			72.08	
48			71.54	
49			70.98	
50			70.38	

<sup>a</sup> Experimental values from Ref. [26,28]<sup>b</sup> Experimental values from Ref. [27]

Our calculations reproduce this global behaviour. It can also be noticed that vibronic shifts differences, taken from [7], assuming they are transferable, present a strong correlation with our error in the vibrational spacing with respect to experiment. For example, for  $v = 0, 2, 3, 4, 5$  vibronic effects are expected to increase the vibrational spacing by a few wavenumbers, as our error does compared to experimental spacing. The effect on the  $v = 6$  level amounts to about

$50\text{ cm}^{-1}$ , resulting in an inversion of levels 6 and 7, and thus reducing the apparent discrepancy that can be seen in Table 4. For  $v = 23$  and  $v = 24$ , vibronic shifts are predicted to increase the spacing by 18 and  $9\text{ cm}^{-1}$ , respectively, while our errors are about 13 and  $9\text{ cm}^{-1}$ . However for a deeper comparison, a diabatic approach consistent with the present adiabatic data should be performed and the vibronic effects reevaluated.

### 3.2 Dipole moments

Permanent electric dipole moments of LiH in the  $X$ ,  $A$ ,  $C$  and  $D$  states are reported in Fig. 5. Here again, the curves have not been interpolated, taking benefit of the large number of calculated points. As emphasised in [23], permanent dipole moments nicely illustrate the ionic character of the adiabatic states. The consecutive crossings  $X$ - $A$ ,  $A$ - $C$  and  $C$ - $D$  are related to the neutral-ionic avoided crossings in the potential energy curves and give a mean to locate with confidence these crossings within an adiabatic approach. Quite similar results were found for the ground state by the all-electron approach of Lundsgaard and Rudolph [34]. For completeness, transition dipole moments from the  $X$  state to  $A$ ,  $C$  and  $D$  states are reported in Fig. 6. The maximum of the  $X$ - $A$  transition dipole is known to be sensitive to the position of the neutral-ionic avoided crossing, for larger distances it rapidly reaches the atomic  $2s - 2p$  asymptotic limit. The two other transition dipole moments are much less intense, the  $X$ - $C$  one changing sign around  $R = 7$  a.u.

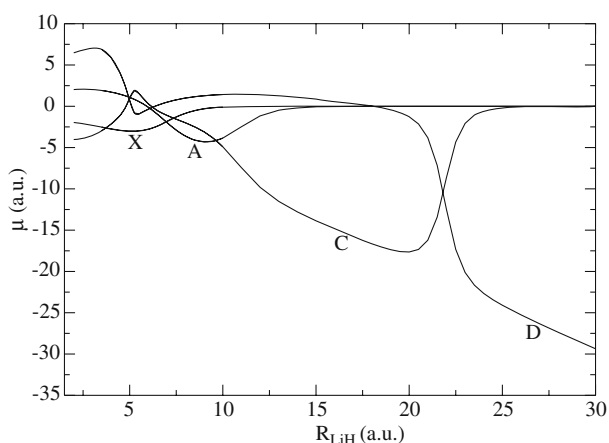


**Fig. 5** Permanent dipole moments of the low-lying  $1\Sigma^+$  states of LiH

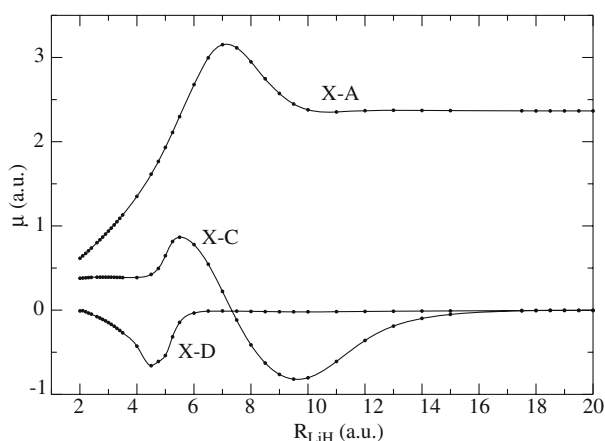


**Fig. 6** Transition dipole moments from the  $X$  to the  $A$ ,  $C$  and  $D$   $1\Sigma^+$  states of LiH

**Table 5** Spacings (in  $\text{cm}^{-1}$ ),  $\Delta G_v^+$ , of  $\text{LiH}^+$

$v$	Lundsgaard and Rudolph <sup>a</sup>	Berriche and Gadea <sup>b</sup>	Present work
0	351.6	357.4	353.9
1	257.2	265.6	260.3
2	163.5	173.0	168.9
3	84.1	92.2	88.3
4	31.8	37.5	34.7
5	7.3	9.2	9.1

<sup>a</sup> Theoretical values from Ref. [34]

<sup>b</sup> Theoretical values from Ref. [37]

## 4 $\text{LiH}^+$

The spectroscopy of  $\text{LiH}^+$  is still unobserved, despite this ion plays an important role in astrophysics chemistry and also in various plasmas. Several calculations have shown that this spectroscopy could be derived from its photoionisation spectrum which is predicted to present both a continuum and a discrete part [36,37,34]. We used here the huge basis set determined previously and which yields IP and EA of both H and Li with an excellent accuracy, with errors of only 1 and  $6\text{ cm}^{-1}$  for the IP and 15 and  $64\text{ cm}^{-1}$  for the EA of H and Li, respectively. As we are mainly interested here in the ground state, we perform an all-electron calculation at the CCSD(T) level. We get seven vibrational levels trapped in the well. Among the previous studies, only two predicted seven vibrational levels, the others found a less deep well with fewer vibrational levels. The former is a pseudopotential approach where the origin of the well was attributed to charge delocalisation due to a strong interaction between the two ionic forms [37]. The second is the all-electron full CI approach cited above [34].

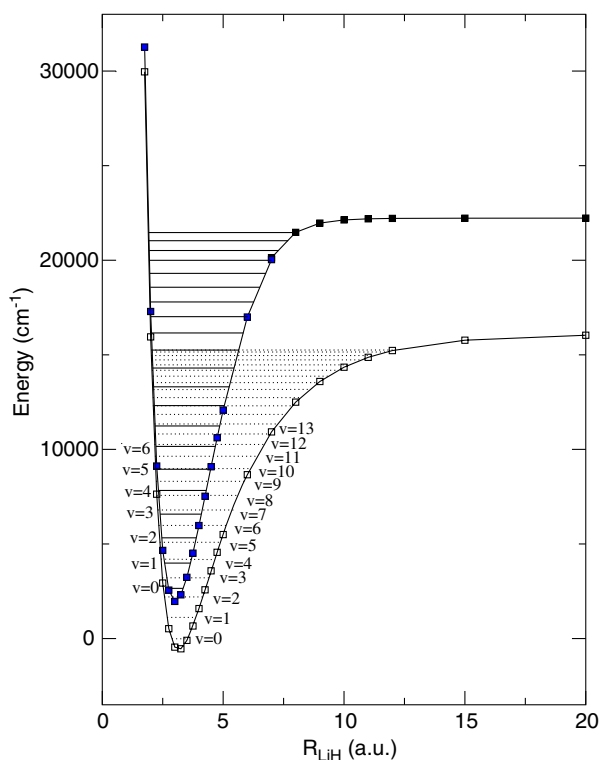
Vibrational spacings, as well as spectroscopic constants resulting from the present work are compared in Table 5 with these two contributions. Our dissociation energy is very closed to the pseudopotential one [37] which also used very large basis set and somewhat larger than the previous all-electron determination [34] which involved a smaller basis set. The equilibrium distance is shorter in the pseudopotential approach while both all-electron calculations find a very similar one. This behaviour follows the general trend for pseudopotential approaches in underestimating the equilibrium distance and overestimating the binding energy. This is consistent with some underestimation of repulsive effects of the pseudopotential approach. However, the equilibrium distance of  $\text{LiH}^+$  is reached at larger interatomic distances compared to LiH and the differences are less important. The rather good agreement between these data gives confidence in the theoretical predictions. We get vibrational spacings intermediate between the two previous calculations. For a three-electron system, CCSD(T) is expected to be very closed to full CI; therefore we are confident that the present work which involves a much larger basis set than the one used in [34] is more accurate.

**Table 6** Spectroscopic constants of the ground state of LiH and LiH<sup>-</sup>, all-electron CCSD(T) calculations

	LiH $X^1\Sigma^+$	LiH <sup>-</sup> $^2\Sigma^+$
$R_e$ (a.u.)	3.015	3.152
$D_e$ (eV)	2.512	2.075
$\omega_e$ (cm <sup>-1</sup> )	1383.2	1167.5
$\omega_e x_e$ (cm <sup>-1</sup> )	-17.7	-25.6

**Table 7** Spacings (in cm<sup>-1</sup>),  $\Delta G_v^+$  between the vibrational levels of the ground state of LiH and LiH<sup>-</sup>, all-electron CCSD(T) calculations

$v$	LiH $^1\Sigma^+$	LiH <sup>-</sup> $^2\Sigma^+$
0	1359.98	1129.22
1	1315.22	1074.15
2	1271.87	1020.83
3	1228.68	969.25
4	1185.69	919.06
5	1143.27	870.18
6	1101.59	822.65
7	1060.62	776.73
8	1020.24	732.58
9	979.98	689.95
10	939.13	648.78
11	897.48	609.04
12	854.93	570.72
13	811.01	533.74
14	764.63	498.25
15	713.71	464.51
16	656.18	432.47
17	589.90	401.47
18	513.45	370.32
19	429.30	338.84

**Fig. 7** Potential energy and vibrational levels of the ground states of LiH and LiH<sup>-</sup>

## 5 LiH<sup>-</sup>

Although calculations for LiH<sup>-</sup> are scarce, the anion has been predicted to be stable relative to LiH, which was confirmed by an experimental observation of the photoelectron spectrum of LiH<sup>-</sup> [38]. An interesting first-principles determination of the photoelectron spectrum of LiH<sup>-</sup> has been reported recently [39], and our present data could be useful in that direction. This study involved all the electrons and was performed at the multireference configuration interaction single and double together with Davidson correction (MRCISD+Q) level. Here again, as we were interested in comparing the ground states of LiH and LiH<sup>-</sup>, we performed for both molecules all-electron calculations at the CCSD(T) level, using the same basis set than previously for H (1 and 15 cm<sup>-1</sup> error in IP and EA, respectively) and a slightly smaller basis set for Li, differing only in the very diffuse exponents devoted to the highest Rydberg states. The resulting vibrational spacing and spectroscopic constants for LiH and LiH<sup>-</sup> are reported in Table 6, while the potentials are illustrated in Fig. 7.

The well for LiH<sup>-</sup> is wider than for LiH and all the vibrational spacings are smaller for the anion than for the neutral molecule. We found three vibrational levels of LiH<sup>-</sup> below the lowest vibrational level of LiH. At least these levels of the anion are stable with respect to autoionisation. At very short distances, the two curves have parallel shapes, indicating that the calculation of the anion has converged to the neutral state and an electron in a diffuse orbital. We could not determine with precision where the two curves crosses. The behaviour of the two curves indicates that this crossing occurs above  $v = 6$  of LiH or equivalently  $v = 13$  of LiH<sup>-</sup>. Therefore the vibrational levels of LiH<sup>-</sup> above  $v = 13$  given in Table 7, are only indicative since their real inner turning point may be in the continuum, and thus correspond to resonances.

It is now interesting to analyse the accuracy of this new neutral potential computed with almost the same huge basis set than in the pseudopotential approach reported in the preceding section, but now with an all-electron approach at the CCSD(T) level. The equilibrium distance is now excellent, with an error less than  $10^{-3}$  a.u., and better than the result of Lundsgaard and Rudolph [34] which underestimated it by at least  $2 \times 10^{-3}$  a.u. The dissociation energy is also largely improved with respect to the previous all-electron calculation which suffers from basis set limitations. Our error compared to the experimental result is only, 24 cm<sup>-1</sup>, an order of magnitude better than the best previous ab initio determination [34]. However, the vibrational spacing of Lundsgaard and Rudolph remains slightly better for the few lowest levels, while globally we get better results which deteriorate only for the highest levels. Our error in the spacing becomes substantially larger than a wavenumber for  $v$  higher than 15, while it was for  $v = 8$  in the previous work [34]. Only for the levels higher than  $v = 15$  the pseudopotential spacing is also



**Table 8** Dissociation limit ( $E_\infty$ ), equilibrium energies ( $E_e$ ) (in Hartree) and transition energies ( $G_0 = E_{v=0} - E_e$  and  $\Delta_{00} = E_{v=0}^{ion} - E_{v=0}^{LiH}$ ) (in  $\text{cm}^{-1}$ ) of LiH, LiH<sup>+</sup> and LiH<sup>-</sup>

	$E_\infty$	$E_e$	$G_0$	$\Delta_{00}$
LiH <sup>+</sup>	-7.779398	-7.784539	211.20	62126.47
LiH	-7.977516	-8.069827	698.21	0
LiH <sup>-</sup>	-8.005165	-8.081439	586.68	-2660.07

better. From these comparisons we can deduce that the calculation of Lundsgaard and Rudolph beneficiates from some error compensations, since the bottom of the well is excellent but slightly shifted in  $R$  and suffers from a smaller basis set as indicated by quite large errors in the EA of H and in the dissociation energy. Our all-electron CCSD(T) approach may suffer near the bottom of the well from the lack of the contribution of quadruple excitations, but globally yields a nice improvement.

As we have performed accurate calculations for the ground states of LiH, LiH<sup>+</sup> and LiH<sup>-</sup>, which are moreover consistent since they used very similar basis sets and identical all-electron approaches at the CCSD(T) level, we report in Table 8 some data corresponding to the absolute and relative position of the minima and lowest vibrational levels. We hope this information could be useful for experiments or further detailed studies. From this table it is easy to deduce that our adiabatic IP and EA ( $\Delta_{00}$ ) of LiH are 7.702762 and 0.329809 eV, respectively. This last value can be compared to the highly accurate specific determination of Bubin and Adamowich [12] 0.33030 eV and to the experimental result  $0.342 \pm 0.012$  eV [38].

## 6 Conclusion

Accurate ab initio calculations have been performed for LiH, LiH<sup>+</sup> and LiH<sup>-</sup>, using huge basis sets; it is almost the same for the three molecules. For LiH, using a pseudopotential approach, a rather complete investigation has been produced for  $1,3\Sigma^+$  potentials and electric dipole moments, involving all potential curves dissociating below the Li(5s)+H(1s) asymptote. It yields very good spectroscopic constants in excellent, previously unattained, agreement with experiment, for the higher part of the  $X$  state and all the  $A$  state. A spectacular agreement, of the order of a tenth of a wavenumber and often much less, is obtained for the  $C$  state with all the experimental level spacings not much affected by vibronic effects. Moreover, the larger disagreements are correlated in sign and in magnitude with the vibronic shift differences. This remarkable agreement shows that the use of huge basis sets yielding accurate asymptotes allows for very good descriptions at intermediate and long distances, while underestimation of repulsive effects arises only at the short interatomic distances. Interestingly, this shows that there is room and need for deriving ab initio results and analysis which could be very accurate and compatible with a diabatic approach. A goal which was an important objective for Jean-Paul Malrieu. This study has

been completed by all-electron calculations at the CCSD(T) level for the ground state of LiH, LiH<sup>+</sup> and LiH<sup>-</sup>. For the neutral molecule, where the results could be compared with the experimental ones, it gives a really remarkable global accuracy, improving all previous ab initio studies. A similar accuracy is expected for the anion and the cation, thus providing useful results, which could motivate further theoretical and experimental work.

**Acknowledgements** We are grateful to Jean-Pierre Daudey for giving us the opportunity of the present contribution, published in honor of Jean-Paul Malrieu.

## References

1. Stwalley WC, Zemke WT (1993) J Phys Chem Ref Data 22:87
2. Mendez L, Cooper IL, Dickinson AS, Mo O, Riera A (1990) J Phys B 23:2797
3. Boutalib A, Gadéa FX (1992) J Chem Phys. 97:1144
4. Gadéa FX, Boutalib A (1993) J Phys B 26:61
5. Gadéa FX, Berriche H, Roncero O, Villarreal P, Delgado Barrio G (1997) J Chem Phys 107:10515
6. Gemperle F, Gadea FX (1999) J Chem Phys 110:11197
7. Gemperle F, Gadea FX (1999) Europhys Lett 48:513
8. Rosmus P, Meyer W (1977) J Chem Phys 66:13
9. Casida ME, Guiterrez F, Guan J, Gadea FX, Salahub D, Daudey JP (2000) J Chem Phys 113:7063
10. Caffarel M, Gadea FX, Ceperley DM (1991) Europhys Lett 16:249
11. Li X, Paldus J (2003) J Chem Phys 118:2470
12. Bubin S, Adamowicz L (2004) J Chem Phys 121:6249
13. Gianturco FA, Gori-Giorgi P, Berriche H, Gadea FX (1996) Astron Astrophys Suppl ser 117:377
14. Stancil PC, Dalgarno A (1997) Astrophys J 479:543
15. Croft H, Dickinson AS, Gadea FX (1999) Mon Notices R Astro Soc 304:327
16. Dickinson AS, Gadea FX (2000) Mon Notices R Astro Soc 318:1227
17. Bodo E, Gianturco FA, Martinazzo R (2003) Phys Rep-Rev Sect Phys Lett 384:85
18. Bennett OJ, Dickinson AS, Leininger T, Gadea FX (2003) Mon Not R Astron Soc 341:361
19. MOLPRO, a package of ab initio programs designed by Werner H-J, Knowles PJ, version 2002.1, with contributions from Amos RD, Bernhardsson A, Berning A, Celani P, Cooper DL, Deegan MJO, Dobbyn AJ, Eckert F, Hampel C, Hetzer G, Knowles PJ, Korona T, Lindh R, Lloyd AW, McNicholas SJ, Manby FR, Meyer W, Mura ME, Nicklass A, Palmieri P, Pitzer R, Rauhut G, Schütz M, Schumann U, Stoll H, Stone AJ, Tarroni R, Thorsteinsson T, Werner H-J, Birmingham, UK, 2002
20. Fuentealba P, Preuss H, Stoll H, Szentpaly LV (1982) Chem Phys Lett 89:418
21. Moore CE (1971) Atomic nergy levels, NBS-NSRDS 35, vol 1, National Bureau of Standards, Department of Commerce, Washington
22. Gadea FX, Leininger T, Dickinson AS (2001) Euro Phys JD 15:251
23. Berriche H, Gadea FX (1995) Chem Phys Lett 24:85
24. Romero T, Aguilar A, Gadea FX (1999) J Chem Phys 110:6219
25. Khelifi N, Zrafi W, Oujia B, Gadea FX (2002) Phys Rev A 65:042513
26. Chen JJ, Luh WT, Jeung GH (1999) J Chem Phys 110:4402
27. Huang YL, Luh WT, Jeung GH, Gadea FX (2000) J Chem Phys 113:683
28. Hsu JK, Wang JJ, Yu R, Wu CY, Luh WT (2002) J Phys Chem 106:6279
29. Bouloufa N, Cabaret L, Vetter R, Luh WT (2004) J Chem Phys 121:7237

30. Gadea FX, Pélissier M (1990) *J Chem Phys* 93:545
31. Croft H, Dickinson AS, Gadea FX (1999) *J Phys B* 32:81
32. Dickinson AS, Gadea FX (2002) *Phys Rev A* 65:052506
33. Dickinson AS, Gadea FX (2003) *J Mol Struct Theochem* 621:87
34. Lundsgaard MFV, Rudolph H (1999) *J Chem Phys* 111:6724
35. Gadea FX, Gemperle F, Berriche H, Villarreal P, Delgado Barrio G (1997) *J Phys B* 3:L427
36. Brabandt O, Bakker HJ, de Lange CA (1992) *Chem Phys Lett* 189:291
37. Berriche H, Gadea FX (1996) *Chem Phys* 203:373
38. Sarkas HW, Hendricks JH, Arnold ST, Bowen KH (1994) *J Chem Phys* 100:1884
39. Chang DT, Reimann K, Surratt G, Gellene GI, Lin P, Lucchese R (2002) *J Chem Phys* 117:5757
40. Gemperle F, Gadea FX, Durand P (1998) *Chem Phys Lett* 291:517
41. Lin WC, Chen JJ, Luh WT (1997) *J Phys Chem A* 10:6709
42. Anderson WR, Veale JR, Gallagher TF (1998) *Phys Rev Lett* 80:249
43. Mourachko I, Comparat D, de Tomasi F, Fioretti A, Nosbaum P, Akulin VM, Pillet P, *Phys Rev Lett* 80:253
44. Born M, Oppenheimer R (1927) *Ann Phys* 84:457
45. Kleinman LI, Wolfsberg M (1974) *J Chem Phys* 60:4740
46. Bishop DM, Cheung LM (1983) *J Chem Phys* 78:1396
47. Jensen JO, Yarkony DR (1986) *J Chem Phys* 89:3853
48. Vidal CR, Stwalley WC (1982) *J Chem Phys* 77:883
49. Chan YC, Harding DR, Stwalley WC, Vidal CR (1986) *J Chem Phys* 85:2436
50. Pacher T, Cederbaum LS, Koeppl H (1993) *Adv Chem Phys* 84:293
51. Corderman RR, Lineberger WC (1979) *Ann Rev Phys Chem* 30:347
52. Hotop H, Lineberger WC (1985) *J Phys Chem Ref Data* 14:731
53. Barat M, Lichten W (1971) *Phys Rev A* 6:211
54. Leininger T, Gadea FX, Dickinson AS (2000) *J Phys B* 33:1805
55. Way KR, Stwalley WC (1973) *J Chem Phys* 5:5298